



## ROCKING ISOLATION OF BLOCK-LIKE OBJECTS UNDER DYNAMIC BASE EXCITATION

P. C. Roussis<sup>1</sup>, E. A. Pavlou<sup>2</sup>, and E. C. Pisiara<sup>3</sup>

### ABSTRACT

This paper presents a study on the rocking isolation of block-like objects under dynamic base excitation. The structural model employed consists of a rigid block supported on a practically-rigid pedestal, beneath which the isolation system is accommodated. The rocking response of the seismically isolated rigid block subjected to base excitation is studied. Assuming no sliding of the block relative to the supporting base, when subjected to ground excitation the system may exhibit two possible patterns of motion, namely pure translation, in which the system in its entirety oscillates horizontally, and rocking, in which the rigid block pivots on its edges with respect to the horizontally-moving base. The dynamic response of the system is strongly affected by the occurrence of impact between the block and the horizontally-moving base, as impact can modify not only the energy but also the degrees of freedom of the system by virtue of the discontinuity introduced in the response. The formulation of the problem involves derivation of the nonlinear equations of motion, transition criteria from one regime of motion to another and an appropriate impact model. Numerical results are obtained via an ad-hoc computational scheme developed to determine the response of the system under horizontal ground excitation.

### Introduction

Thus far particular attention has been given to the application of seismic isolation in earthquake engineering to safeguard the primary structural system in bridges, buildings and the infrastructure. On the contrary, limited attention has been given to the application of base-isolation technology to individual elements, such as building contents, mechanical and electrical equipment, computer servers, statues and other objects of great value and importance. To this end, this study serves to expand the knowledge on the dynamic behavior of base-isolated rigid bodies by exploiting the potential of seismic-isolation strategy to mitigate their seismic risk.

In the literature, there is a wealth of research papers on the seismic behavior of block-like structures. Housner's landmark study (Housner 1963) has provided the basic understanding on the rocking response of a slender rigid block and sparked modern scientific interest. His model is based on the assumption of perfectly-inelastic impact and sufficient friction to prevent sliding during impact. Following Housner's fundamental work, numerous studies (e.g. Yim et al. 1980, Ishiyama 1982, Spanos and Koh 1984, Shenton and Jones 1991, Makris and Roussos 2000) have been

<sup>1</sup> Assistant Professor, Dept. of Civil & Environmental Engineering, University of Cyprus, Nicosia, Cyprus

<sup>2</sup> Research Associate, Dept. of Civil & Environmental Engineering, University of Cyprus, Nicosia, Cyprus

<sup>3</sup> Graduate Student, Dept. of Civil & Environmental Engineering, University of Cyprus, Nicosia, Cyprus

reported in the literature dealing with various aspects of the complex dynamics of the single rigid block. Studies have also been conducted on the non-linear dynamic response of systems consisting of two blocks, one placed on top of the other, free to rock without sliding (e.g. Spanos et al. 2001).

This paper presents a study on the rocking response of base-isolated block-like objects under dynamic base excitation. The structural model employed consists of a rigid block supported on a practically-rigid pedestal, beneath which the isolation system is accommodated. Assuming no sliding of the block relative to the supporting base, when subjected to ground excitation the system may exhibit two possible patterns of motion, namely pure translation, in which the system in its entirety oscillates horizontally, and rocking, in which the rigid block pivots on its edges with respect to the horizontally-moving base. The dynamic response of the system is strongly affected by the occurrence of impact between the block and the horizontally-moving base, as impact can modify not only the energy but also the degrees of freedom of the system by virtue of the discontinuity introduced in the response. The formulation of the problem involves derivation of the nonlinear equations of motion, transition criteria from one regime of motion to another and an appropriate impact model. Numerical results are obtained via an ad hoc computational scheme developed to determine the response of the system under horizontal ground excitation.

## Analytical Model

### Model Considered

The system considered consists of a symmetric rigid block of mass  $m$  and centroid mass moment of inertia  $I$ , supported on a horizontal rigid foundation (Fig. 1). The rigid block of height  $H = 2h$  and width  $B = 2b$  is assumed to rotate about the base corners  $O$  and  $O'$ . The distance between one corner of its base and the mass center is denoted by  $r$  and the angle measured between  $r$  and the vertical when the body is at rest is denoted by  $\alpha$ , where  $\alpha = \tan^{-1}(b/h)$ .

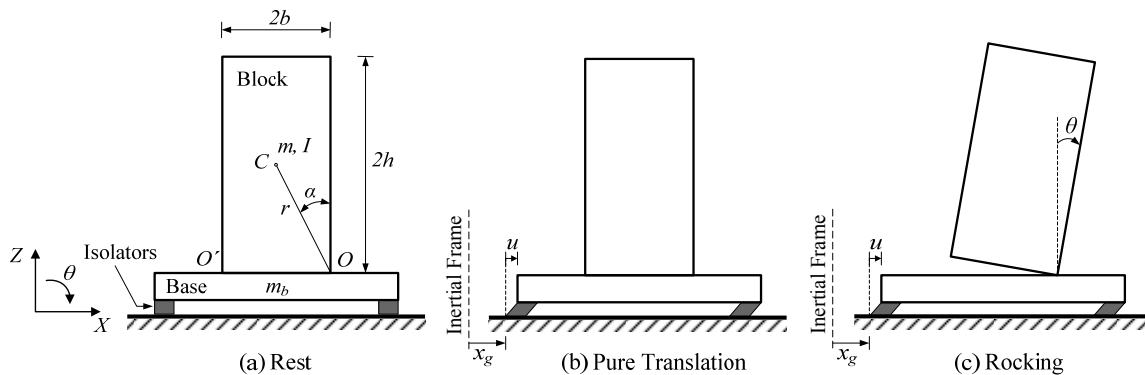


Figure 1. Model at rest and oscillation patterns

The horizontal and vertical displacements of the mass center of the block relative to an inertial frame of reference are denoted by  $X(t)$  and  $Z(t)$  respectively, while the corresponding

displacements relative to the base are denoted by  $x(t)$  and  $z(t)$ . The angular rotation of the block is denoted by  $\theta(t)$ , positive in the clockwise direction, and the horizontal displacement of the base relative to the foundation is denoted by  $u(t)$ .

## Equations of Motion

Assuming no sliding of the block relative to the supporting base, when subjected to ground excitation the system may exhibit two possible patterns of motion: (a) pure translation, in which the system in its entirety oscillates horizontally with displacement  $u(t)$  (1 degree-of-freedom response), and (b) rocking, in which the rigid block pivots on its edges with rotation  $\theta(t)$  as the supporting base translates horizontally with  $u(t)$  (2 degree-of-freedom response). The governing equations for each pattern of motion are herein formulated by means of the Lagrange method.

### *Pure-translation regime*

The equation of motion of the system in the pure-translation regime is

$$(m + m_b)\ddot{u} + c\dot{u} + ku = -(m + m_b)\ddot{x}_g \quad (1)$$

which is the classical linear second-order differential equation governing the response of a single-degree-of-freedom system to ground excitation.

### *Rocking regime*

In the rocking regime the system possesses two degrees of freedom. Using as generalized coordinates the horizontal translation of the base relative to the ground,  $u$ , and the rotation angle of the object about a bottom corner,  $\theta$ , Lagrange's equations take the form

$$\frac{d}{dt}\left(\frac{\partial T}{\partial \dot{u}}\right) - \frac{\partial T}{\partial u} + \frac{\partial V}{\partial u} = Q_u \quad \text{and} \quad \frac{d}{dt}\left(\frac{\partial T}{\partial \dot{\theta}}\right) - \frac{\partial T}{\partial \theta} + \frac{\partial V}{\partial \theta} = Q_\theta \quad (2)$$

in which  $T$  denotes the kinetic energy of the system,  $V$  the potential energy of the system, and  $Q_u$ ,  $Q_\theta$  the generalized nonconservative forces.

The kinetic energy of the system is obtained as

$$T = \frac{1}{2}m_b(\dot{u} + \dot{x}_g)^2 + \frac{1}{2}m\left[(\dot{u} + \dot{x}_g + h\dot{\theta}\cos\theta + b\dot{\theta}\sin\theta)^2 + (b\dot{\theta}\cos\theta - h\dot{\theta}\sin\theta)^2\right] + \frac{1}{2}I\dot{\theta}^2 \quad (3)$$

in which the first term is associated with pure translation of the base, and the second and third term are associated with general planar motion of the block.

The potential energy of the system is obtained as

$$V = \frac{1}{2}ku^2 + mg[b\sin\theta - h(1 - \cos\theta)] \quad (4)$$

in which the first term is associated with the potential energy due to elastic deformation of the spring and the second term is associated with the potential energy due to gravity.

The generalized forces are derived via the virtual work of the nonconservative forces as

$$Q_u = -c\dot{u}, \quad Q_\theta = 0 \quad (5)$$

Substituting Eqs. (3) through (5) into Eq. (2) yields the governing equations of motion for rotation about  $O$  ( $\theta > 0$ ). The governing equations of motion for rotation about  $O'$  ( $\theta < 0$ ) can be derived in a similar manner. Combining the equations for rotation about  $O$  and  $O'$ , leads to a compact set of equations governing the rocking regime of the object on top of the moving base:

$$(m+m_b)\ddot{u} + c\dot{u} + ku + m[h\cos\theta + \text{sgn}\theta(b\sin\theta)]\ddot{\theta} + m[\text{sgn}\theta(b\cos\theta) - h\sin\theta]\dot{\theta}^2 = -(m+m_b)\ddot{x}_g \quad (6)$$

$$(mr^2 + I)\ddot{\theta} + m\dot{u}[h\cos\theta + \text{sgn}\theta(b\sin\theta)] + mg[\text{sgn}\theta(b\cos\theta) - h\sin\theta] = -m[h\cos\theta + \text{sgn}\theta(b\sin\theta)]\ddot{x}_g \quad (7)$$

where  $\text{sgn}\theta$  denotes the signum function in  $\theta$ . Note that Eqs. (6) and (7) hold only in the absence of impact ( $\theta \neq 0$ ). At that instant, both corner points  $O$  and  $O'$  are in contact with the base, rendering the above formulation invalid. The impact problem is addressed separately in the following section.

### Impact Model

The dynamic response of the system is strongly affected by the occurrence of impact(s) between the block and the horizontally-moving base. In fact, impact affects the system response on many different levels. On one level, it renders the problem nonlinear (aside from the nonlinear nature of the equations themselves) by virtue of the discontinuity introduced in the response (i.e. the governing equations of motion are not valid for  $\theta = 0$ ). That is, impact causes the system to switch from one oscillation pattern to another (potentially modifying the degrees of freedom), each one governed by a different set of differential equations. Further, the integration of equations of motion governing the post-impact pattern must account for the ensuing instantaneous change of the system's velocity regime. On another level, the effect of impact on the dynamic response is also evident in the energy loss of the system manifested through the reduction of post-impact velocities.

Therefore, the critical role of impact in the dynamics of the system necessitates a rigorous formulation of the impact problem. In this paper a model governing impact is derived from first principles using classical impact theory. According to the principle of impulse and momentum, the duration of impact is assumed short and the impulsive forces are assumed large relative to other forces in the system. Changes in position and orientation are neglected, and changes in velocity are considered instantaneous. Moreover, this model assumes a point-impact,

zero coefficient of restitution (perfectly inelastic impact), impulses acting only at the impacting corner (impulses at the rotating corner are small compared to those at the impacting corner and are neglected), and sufficient friction to prevent sliding of the block during impact.

Under the assumption of perfectly inelastic impact, there are only two possible response mechanisms following impact: (a) rocking about the impacting corner when the block re-uplifts (no bouncing), or (b) pure translation when the block's rocking motion ceases after impact. The formulation of impact is divided into three phases: pre-impact, impact, and post-impact as illustrated schematically in Fig. 2. In the following, a superscript “-” refers to a pre-impact quantity and a superscript “+” to a post-impact quantity.

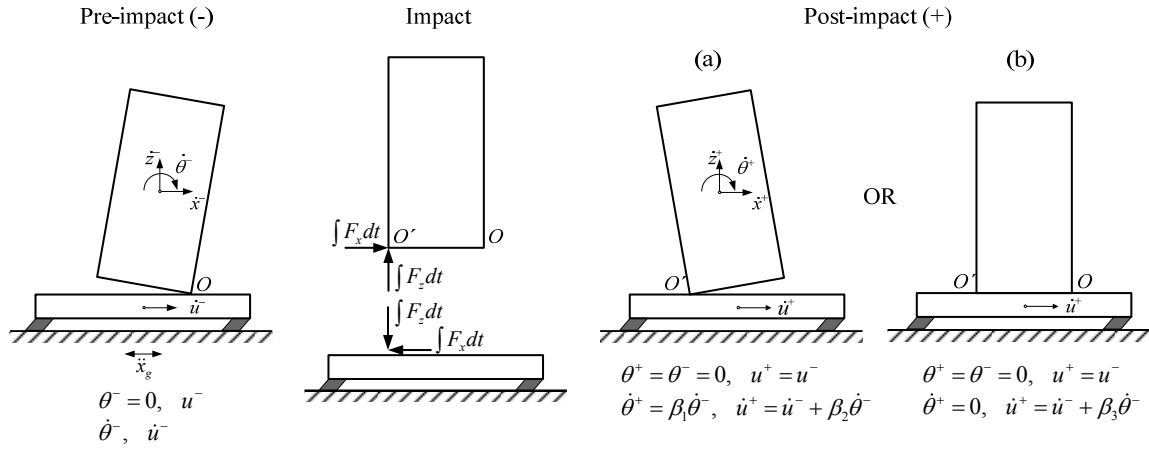


Figure 2. Impact from rocking about  $O$  followed by (a) re-uplift about  $O'$  and (b) termination of rocking

### Rocking continues after impact

Consider the system at the instant when the block hits the moving base from rocking about  $O$  and re-uplifts pivoting about the impacting corner,  $O'$  (Figure a). As mentioned before, impact is accompanied by an instantaneous change in velocities, with the system displacements being unchanged. Therefore, the impact analysis is reduced to the computation of the initial conditions for the post-impact motion,  $\dot{u}^+$  and  $\dot{\theta}^+$ , given the position and the pre-impact velocities,  $\dot{u}^-$  and  $\dot{\theta}^-$ .

With regard to the block, the principle of linear impulse and momentum in the  $x$  and  $z$  direction states that

$$\int F_x dt = m\dot{X}^+ - m\dot{X}^- = m\dot{u}^+ + m\dot{x}^+ - m\dot{u}^- - m\dot{x}^- \quad (8)$$

$$\int F_z dt = m\dot{Z}^+ - m\dot{Z}^- = m\dot{z}^+ - m\dot{z}^- \quad (9)$$

in which  $\int F_x dt$  and  $\int F_z dt$  are the horizontal and vertical impulses (assumed to act at  $O'$ );

$\dot{X}^- = \dot{u}^- + \dot{x}_g^- + \dot{x}^-$ ,  $\dot{X}^+ = \dot{u}^+ + \dot{x}_g^+ + \dot{x}^+$  and  $\dot{Z}^- = \dot{z}^-$ ,  $\dot{Z}^+ = \dot{z}^+$  are the absolute pre- and post-impact horizontal and vertical velocities of the mass center of the block, respectively.

In addition, the principle of angular impulse and momentum states that

$$b\left(\int F_z dt\right) - h\left(\int F_x dt\right) = I\dot{\theta}^+ - I\dot{\theta}^- \quad (10)$$

in which for rectangular block the centroid mass moment of inertia  $I = m(b^2 + h^2)/3$ .

In Eqs. (8) and (9), the pre- and post-impact horizontal and vertical components of the relative translational velocity of the mass center can be expressed in terms of the angular velocity of the block as

$$\dot{x}^- = h\dot{\theta}^-, \quad \dot{z}^- = b\dot{\theta}^-, \quad \dot{x}^+ = h\dot{\theta}^+, \quad \dot{z}^+ = -b\dot{\theta}^+ \quad (11)$$

Substituting Eqs. (11) into Eqs. (8) and (9) yields

$$\int F_x dt = m\dot{u}^+ + mh\dot{\theta}^+ - m\dot{u}^- - mh\dot{\theta}^- \quad (12)$$

$$\int F_z dt = -mb\dot{\theta}^+ - mb\dot{\theta}^- \quad (13)$$

One additional equation is therefore required to uniquely determine the post-impact velocities  $\dot{\theta}^+$  and  $\dot{u}^+$ . By considering the system in its entirety during the impact, it can be stated that the horizontal impulse on the system is zero, resulting in the conservation of the system's linear momentum in the horizontal direction. That is,

$$(m_b + m)\dot{u}^+ = (m_b + m)\dot{u}^- - mh\dot{\theta}^+ + mh\dot{\theta}^- \quad (14)$$

Combining Eqs. (10), (12), (13) and (14) gives the post-impact velocities as

$$\dot{\theta}^+ = \frac{\lambda^2(\bar{m} + 4) - 2(\bar{m} + 1)}{\lambda^2(\bar{m} + 4) + 4(\bar{m} + 1)}\dot{\theta}^- \equiv \beta_1\dot{\theta}^- \quad (15)$$

and

$$\dot{u}^+ = \dot{u}^- + \frac{6\bar{m}h}{\lambda^2(\bar{m} + 4) + 4(\bar{m} + 1)}\dot{\theta}^- \equiv \dot{u}^- + \beta_2\dot{\theta}^- \quad (16)$$

in which  $\lambda = h/b$  is the geometric aspect ratio and  $\bar{m} = m/m_b$  is the mass ratio.

Eqs. (15) and (16) give the post-impact velocities for impact from rocking about  $O$  (realized when  $\dot{\theta} < 0$ ). Identical expressions are derived for the case of impact from rocking

about  $O'$  (realized when  $\dot{\theta} > 0$ ).

It is worth noting that the coefficient of restitution  $e$  as defined in classical impact theory, relates pre- to post-impact *translational* velocities normal to the impact surface, and hence it must not be confused with the coefficient of “angular restitution”  $\beta_1$  defined in Eq. (15), which relates the pre- to post-impact *angular* velocities of the body. In the derivation presented herein, the coefficient of restitution  $e$  enters in the expression  $\dot{z}_{O'}^+ = -e\dot{z}_{O'}^-$ , which relates pre- to post-impact vertical relative velocities of the impacting corner ( $O'$ ). The assumption of perfectly inelastic impact is then justified by considering  $e = 0$ .

From Eq. (15), it can be seen that the coefficient of angular restitution,  $\beta_1$ , depends both on the geometric aspect ratio  $\lambda$  and the mass ratio  $\bar{m}$ . The variation of coefficient  $\beta_1$  with the slenderness ratio  $\lambda$  is shown in Fig. 3a for different values of the mass ratio  $\bar{m}$ . The dependency of coefficient  $\beta_1$  on the mass ratio  $\bar{m}$  is seen to be weak, and practically diminishes for very slender blocks (e.g. for  $\lambda > 6$ ). The value  $\beta_1 = 1$ , implying preservation of the magnitude of the angular velocity after impact, presents an upper bound for the coefficient of angular restitution. Evidently, the more slender a block, the larger the associated coefficient  $\beta_1$  is. For the assumption of *no-bouncing* to be satisfied, the coefficient of angular restitution  $\beta_1$  should have a positive value. In such a case, the angular velocity of the block will maintain sign upon impact, implying switching pole of rotation from one corner to the other. This requires that  $\lambda > \sqrt{2(\bar{m} + 1)/(\bar{m} + 4)}$ .

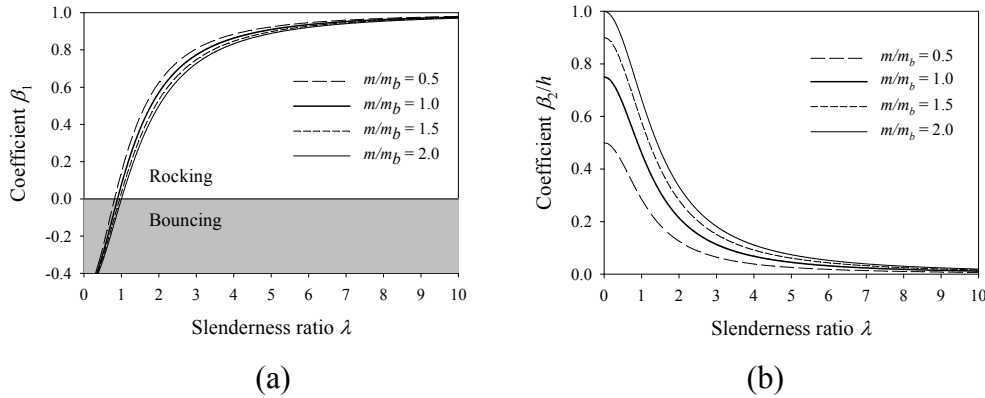


Figure 3. Variation of coefficients  $\beta_1$  and  $\bar{\beta}_2$  with slenderness ratio

The coefficient associated with the reduction of the linear velocity of base,  $\beta_2$ , depends not only on the parameters  $\lambda$  and  $\bar{m}$ , but also on the absolute size of the block (in terms of its height). The normalized coefficient  $\bar{\beta}_2 \equiv \beta_2/h$  is plotted against the slenderness ratio  $\lambda$  for different values of the mass ratio  $\bar{m}$  in Fig. 3b. Observe that the value of the coefficient  $\bar{\beta}_2$  decays rapidly with the slenderness ratio  $\lambda$ . Moreover, the influence of the mass ratio  $\bar{m}$  on the coefficient  $\bar{\beta}_2$  is much greater than that on the coefficient  $\beta_1$ .

## Rocking ceases after impact

When rocking of the block on top of the moving base ceases, the system will attain a pure-translation regime (Fig. 2b). In this case, the impact analysis is reduced to the computation of the post-impact translational velocity of the system,  $\dot{u}^+$ , given the position and the pre-impact velocities,  $\dot{u}^-$  and  $\dot{\theta}^-$ .

By considering the system as a whole during impact, it can be stated that the horizontal impulse on the system is zero, resulting in the conservation of the system's linear momentum in the horizontal direction. That is,

$$m_b(\dot{u}^- + \dot{x}_g) + m(\dot{u}^- + \dot{x}_g + h\dot{\theta}^-) = m_b(\dot{u}^+ + \dot{x}_g) + m(\dot{u}^+ + \dot{x}_g) \quad (17)$$

which upon rearranging terms becomes

$$\dot{u}^+ = \dot{u}^- + \frac{\bar{m}h}{(1+\bar{m})}\dot{\theta}^- \equiv \dot{u}^- + \beta_3\dot{\theta}^- \quad (18)$$

## Numerical Solution

Numerical results were obtained through an ad-hoc computational scheme developed to determine the response of the system under horizontal ground excitation. The numerical integration of the equations of motion was pursued in MATLAB through a state-space formulation (MATLAB 2006). In each time step, close attention is paid to the eventuality of transition from one pattern of motion to another and to the accurate evaluation of the initial conditions for the next pattern of oscillation, on the basis of the developed impact model. To illustrate the practical application of the developed computational scheme, the response of the system under earthquake excitation has been calculated for various system parameters.

The program was executed to calculate the response of a base-isolated rigid block subjected to the N-S component of 1940 El Centro earthquake and the N-S component of 1995 Kobe, Japan earthquake. Results are presented here for certain specific values of various system parameters, including the mass ratio  $\bar{m} = m/m_b$ , slenderness ratio  $\lambda = h/b$ , and size of the rocking block in terms of its half-diameter  $r$ . The linear isolation system considered has period  $T = 1.5$  sec and viscous damping ratio  $\xi = 0.20$ . The response under the same ground excitations was also calculated for the case of the non-isolated block for comparison purposes.

Figs. 4 and 5 present the response of isolated and non-isolated rigid blocks under the selected excitations, in terms of the rotation and angular-velocity time histories of the rigid block. In addition, these figures present the horizontal-displacement history of the base of the isolated block. Comparison between the isolated and non-isolated cases reveals the benefits of the isolation method. It is indicative that rocking of the block in Fig. 4 is prevented entirely with the application of seismic isolation. Even when the non-isolated block exhibits excessive rotation amplitudes, occasionally leading to overturning of the block (e.g. for  $\lambda=5.0$ ,  $\bar{m}=1$ ,  $r=1$  m), the



isolated block remains in full contact with the base, thus yielding linear sdof system response.

Under certain conditions, rocking of the isolated block may be initiated and sustained for a period of time, as shown in Fig. 5. Comparison of the rocking response of the isolated and non-isolated block shows the beneficial effect of seismic isolation in reducing the rotation amplitude, the number of impacts and the overall duration of oscillation. However, the same conclusion cannot be derived for the angular velocity of the block, as its magnitude is found to be comparable for the two cases, with and without isolation. In terms of the rotation amplitude and the number of impacts, compared to the non-isolated block, which is on the verge of overturning ( $|\theta/a|_{\max} = 0.95$ ), the isolated block exhibits a maximum rotation amplitude  $|\theta/a|_{\max} = 0.64$  and as many as 5 times less impacts.

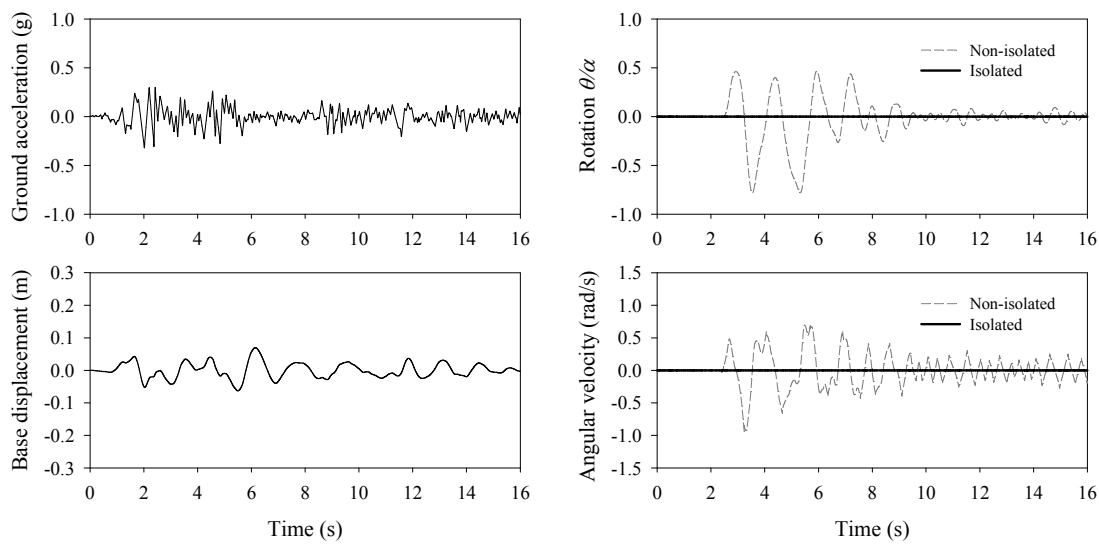


Figure 4. Response of the system to the N-S component of 1940 El Centro earthquake (system parameters:  $\lambda=4.0$ ,  $\bar{m}=1$ ,  $r=1$  m).

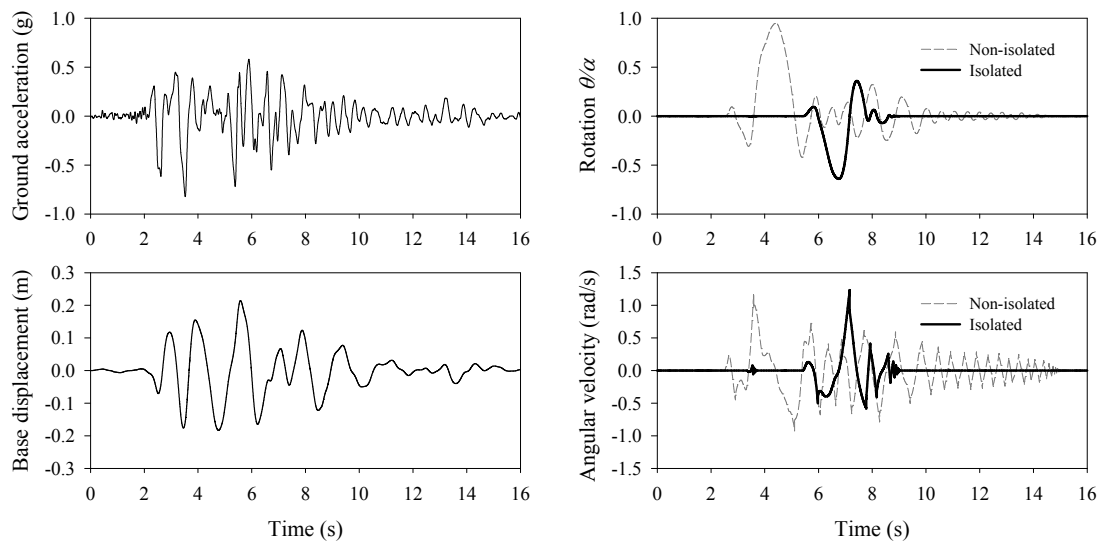


Figure 5. Response of the system to the N-S component of 1995 Kobe, Japan earthquake (system parameters:  $\lambda=2.86$ ,  $\bar{m}=1$ ,  $r=1$  m).

Fig. 6 reports results of an extensive numerical investigation of a class of rigid blocks with different geometric characteristics in terms of the slenderness ratio  $\lambda$  and size of the block  $r$ , for both the non-isolated and isolated case. A total of twelve-hundred nonlinear dynamic analyses were performed in constructing the two behavior maps. Each dot in these maps represents the outcome of a single analysis. The blue circles indicate “No Rocking”, the green “Rocking”, and the red circles “Overturning” of the block. The comparison between the two maps reveals the benefits of the isolation method. Evidently, for the case of the isolated block, the initiation of rocking (boundary between the blue and green areas) is shifted towards higher values of slenderness ratio  $\lambda$  and the instability region (indicated in red) is substantially reduced.

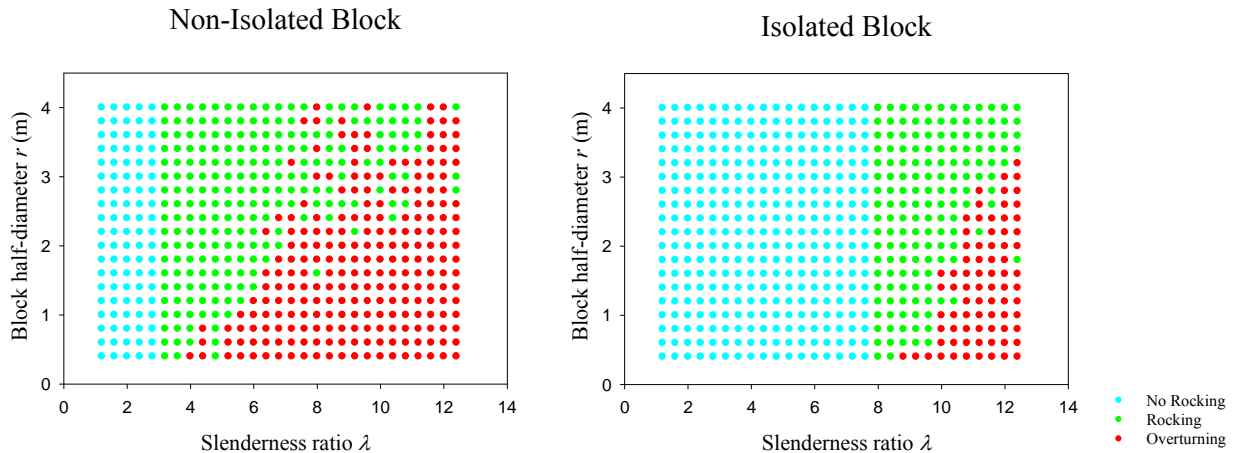


Figure 6. Behavior maps for a class of rigid blocks under the N-S component of 1940 El Centro earthquake ( $\bar{m}=1$ ,  $T_s = 1.5$  s,  $\xi = 20\%$ )

Also, an interesting observation is that, contrary to what intuition would suggest, there seems to be a scale effect. In other words, between two blocks of the same proportion (same  $\lambda$ ) but of different size (different  $r$ ), the larger one is more stable than the smaller. This trend is more evident in the case of the isolated block.

### Concluding Remarks

The rocking response of base-isolated block-like objects under horizontal ground excitation was examined within the context of rigid-body dynamics. The analytical formulation of this highly-nonlinear problem is quite challenging. Its complexity stems primarily from the fact that the dynamics of the system is drastically changed by the occurrence of impact, aside from the nonlinear nature of the governing equations themselves.

The model considered consists of a rigid block supported on a rigid base, beneath which the isolation system is placed. Under the assumption of sufficient friction to prevent sliding of the block relative to the supporting base, when subjected to base excitation the system may exhibit two possible patterns of motion, each being governed by highly nonlinear differential equation(s). The system can be set in pure translation, in which the system as a whole oscillates horizontally (1-DOF response), or rocking, in which the rigid block pivots on its edges with respect to the horizontally-moving base (2-DOF response). In addressing the critical role of

impact in the dynamics of the system, a rigorous formulation of the impact problem using classical impact theory was presented in this paper. Numerical results were obtained via an ad-hoc computational scheme developed to determine the response of the system under horizontal excitation. Results were obtained in order to verify the applicability of the isolation system and to evaluate the influence of its characteristic parameters. The results show that base isolation may effectively be applied to mitigate the rocking response of block-like objects during earthquakes.

## References

Housner G. W., 1963. The behavior of inverted pendulum structures during earthquakes, *GSW Bulletin of the Seismological Society of America*, 53(2), 403-417.

Ishiyama, Y., 1982. Motions of rigid bodies and criteria for overturning by earthquake excitations, *Earthquake Engineering and Structural Dynamics* 10: 635-650.

Makris, N., and Y. S. Roussos, 2000. Rocking response of rigid blocks under near-source ground motions, *Géotechnique* 50: 3, 243-262.

MATLAB 7.3, 2006. *The Language of Technical Computing* The Mathworks, Inc.: Natick, MA.

Shenton III, H. W., and N. P. Jones, 1991. Base excitation of rigid bodies. I: Formulation, *Journal of Engineering Mechanics (ASCE)* 117: 10, 2286-2306.

Spanos, P. D., and A-S Koh, 1984. Rocking of rigid blocks due to harmonic shaking, *Journal of Engineering Mechanics (ASCE)* 110: 11, 1627-1642.

Spanos, P. D., P. C. Roussis, and N. P. Politis, 2001. Dynamic analysis of stacked rigid blocks, *Soil Dynamics and Earthquake Engineering* 21, 559-578.

Yim, C-S, A. K. Chopra, and J. Penzien, 1980. Rocking response of rigid blocks to earthquakes, *Earthquake Engineering and Structural Dynamics* 8: 6, 565-587.